THE COMPANY OF
Biologists

RESEARCH ARTICLE

Planar covariation of limb elevation angles during bipedal locomotion in common quails (*Coturnix coturnix*)

Naomichi Ogihara[1,*], Takaaki Oku[1], Emanuel Andrada[2], Reinhard Blickhan[2], John A. Nyakatura[3] and Martin S. Fischer[3]

ABSTRACT

In human bipedal walking, temporal changes in the elevation angle of the thigh, shank and foot segments covary to form a regular loop within a single plane in three-dimensional space. In this study, we quantified the planar covariation of limb elevation angles during bipedal locomotion in common quails to test whether the degree of planarity and the orientation of the covariance plane differ between birds, humans and Japanese macaques as reported in published accounts. Five quails locomoted on a treadmill and were recorded by a lateral X-ray fluoroscopy. The elevation angle of the thigh, shank and foot segments relative to the vertical axis was calculated and compared with published data on human and macaque bipedal locomotion. The results showed that the planar covariation applied to quail bipedal locomotion and planarity was stronger in quails than in humans. The orientation of the covariation plane in quails differed from that in humans, and was more similar to the orientation of the covariation plane in macaques. Although human walking is characterized by vaulting mechanics of the body center of mass, quails and macaques utilize spring-like running mechanics even though the duty factor is >0.5. Therefore, differences in the stance leg mechanics between quails and humans may underlie the difference in the orientation of the covariation plane. The planar covariation of inter-segmental coordination has evolved independently in both avian and human locomotion, despite the different mechanical constraints.

KEY WORDS: Kinematics, Inter-segmental coordination, Human, Macaque, Grounded running

INTRODUCTION

In human bipedal walking, temporal changes in the elevation angle of the thigh, shank and foot segments, i.e. changes in the orientation of these segments with respect to the vertical axis, covary to form a regular loop within a single plane in three-dimensional space (Borghese et al., 1996; Bianchi et al., 1998; Grasso et al., 1998; Ivanenko et al., 2002; Ivanenko et al., 2005; Ivanenko et al., 2007; Ivanenko et al., 2008; Hicheur et al., 2006; Barliya et al., 2009; Dominici et al., 2010; Ogihara et al., 2012; Sylos-Labini et al., 2013). In humans, the plane can account for more than 99% of the total variance in the elevation angles (Borghese et al., 1996). Such planarity has been observed in a variety of walking conditions, including backward walking (Grasso et al., 1998), walking with

body-weight support (Ivanenko et al., 2002), walking on inclined surfaces (Noble and Prentice, 2008), prosthetic walking (Leurs et al., 2012) and walking in simulated reduced gravity (Sylos-Labini et al., 2013). The planar covariation is thought to simplify the control of human bipedal walking by coordinating kinematic synergies, thus reducing the number of effective degrees of freedom that require control from three to two (Ivanenko et al., 2007; Ivanenko et al., 2008). Humans have acquired a high degree of intersegmental coordination over the course of evolution, possibly to facilitate the control of bipedal walking by reducing the number of degrees of freedom that need to be controlled (Ogihara et al., 2012).

Birds are also exclusively bipedal when they are on the ground. Birds evolved from theropod dinosaur ancestors who are considered to be exclusively bipedal (e.g. Hutchinson and Gatesy, 2001). The history of bipedal locomotion in living birds is therefore much longer (at least 235 million years) than that of human bipedal locomotion (ca. 7 million years). There are large differences in hindlimb anatomy and gait kinematics between birds and humans, and it is not known whether a strong planarity is present in obligate bipedal locomotion in birds. Answering this question may provide insight into the origin and functional significance of the planar covariation in human bipedal locomotion. A large number of experimental studies have been conducted to quantify the kinematics of bird bipedal locomotion (e.g. Gatesy and Biewener, 1991; Muir et al., 1996; Gatesy, 1999; Abourachid and Renous, 2000; Fujita, 2004; Hancock et al., 2007; Rubenson et al., 2007; Nyakatura et al., 2012), including that of quails (e.g. Reilly, 2000; Abourachid et al., 2011; Stoessel and Fischer, 2012; Andrada et al., 2013), but analysis of the planar covariation of limb elevation angles has not been reported yet.

In the present study, we quantified the planar covariation of the thigh, shank and foot elevation angles during bipedal locomotion in quails, *Coturnix coturnix* (Linnaeus 1758), and compared our data with previously published data from human bipedal locomotion and Japanese macaque, *Macaca fuscata* Blyth 1875, bipedal locomotion (Ogihara et al., 2012). We included the comparison with the macaque as the facultative bipedalism in a non-human quadrupedal primate might be situated at an intermediate stage between bird and human bipedal locomotion.

RESULTS

Means and standard deviations of gait parameters and the number of gait cycles analyzed for each subject and velocity are listed in Table 1. Gait speeds of 0.4, 0.6 and 0.75 m s^{-1} corresponded to a Froude number (*Fr*) of about 0.2, 0.4 and 0.6, respectively. Fig. 1 shows a two-dimensional view of the mean elevation angle profile of the thigh, shank and foot segments plotted against the gait cycle for quails (Fig. 1A), humans (Fig. 1B) and macaques (Fig. 1C). Elevation angles were defined such that an increase indicated counter-clockwise rotation of the segment. As shown in Fig. 1, the

[1]Department of Mechanical Engineering, Faculty of Science and Technology, Keio University, Yokohama 223-8522, Japan. [2]Science of Motion, Institut für Sportwissenschaft, Friedrich-Schiller-Universität Jena, 07749 Jena, Germany. [3]Institut für Spezielle Zoologie und Evolutionsbiologie mit Phyletischem Museum, Friedrich-Schiller-Universität Jena, 07743 Jena, Germany.

*Author for correspondence (ogihara@mech.keio.ac.jp)

The Journal of Experimental Biology

> **List of symbols and abbreviations**
> CoM   body center of mass
> Fr Froude number
> r correlation coefficient
> u_{it}, u_{is} and u_{if} direction cosines of the ith eigenvector with the positive axis of the thigh, shank and foot elevation angles, respectively
> $\Delta\varphi_{FS}$ phase shift in elevation angle between the foot and the shank
> $\Delta\varphi_{ST}$ phase shift in elevation angle between the shank and the thigh

elevation angle profiles of quails resembled those of macaques more than they resembled those of humans. Specifically, the shank elevation angle was smaller in quails and macaques than in humans, and the foot elevation angle decreased soon after foot contact in quails and macaques but remained almost constant until the mid-stance phase in humans. The thigh elevation angle was much larger in quails than in humans and macaques, and the range of motion was much smaller, indicating that the thigh segment was situated in a more pronograde (horizontal) posture and the orientation was relatively unchanged throughout the gait cycle in quail bipedal locomotion.

Fig. 2 shows a three-dimensional view of the elevation angles of two quails (subjects 1 and 2) locomoting at 0.4, 0.6 and 0.75 m s⁻¹ ($Fr\approx0.2$, 0.4 and 0.6, respectively), one human locomoting at 6 km h⁻¹ (1.7 m s⁻¹, Fr=0.33) and one macaque locomoting at 4 km h⁻¹ (1.1 m s⁻¹, Fr=0.4). The trajectories progress in the counter-clockwise direction and foot contact corresponds to the top of the loops. The best-fitted planes of the corresponding loop trajectories are also illustrated. Table 2 presents the eigenvectors of the covariance matrix of the elevation angles plotted in Fig. 2 and the percentage variance accounted for by each eigenvector. In quails, the variance accounted for by the first and second eigenvectors was larger than 99% for all subjects and all speeds, indicating that planar coupling of limb segment motions was present during bipedal locomotion in quails. The percentage variance of the third eigenvector (residual variance not accounted for by planar regression) was significantly higher in quails (>99.5%) than in humans (98.2–99.3%; P<0.01 for all combinations), indicating that planar covariation of limb segment motion in quails was more tightly coupled than that in humans; but that in macaques was comparatively weaker (<98.6%) (Ogihara et al., 2012). The orientation of the best-fitting plane of the loop trajectories was substantially different in quails and humans, but similar in quails and macaques (Fig. 2, Table 2) (Ogihara et al., 2012). Comparisons of eigenvectors for quail, human and macaque locomotion indicated that the first eigenvector was similar in all three species (Table 2) (Ogihara et al., 2012). However, the direction cosines of the second eigenvector were significantly different between quails and humans

(P<0.001 for all combinations), resulting in a difference in the plane orientation between the two species. The change in plane orientation with increasing speed was very small in both quails and humans (Bianchi et al., 1998; Ivanenko et al., 2008).

In quails, the mean percentage variance accounted for by the first and second eigenvectors was ~89–92% and 8–11%, respectively (Table 2). The corresponding values are 84–90% and 9–15% in humans and 92–93% and 5–6% in macaques (Ogihara et al., 2012). The values of quail bipedal locomotion were therefore intermediate between those of human and macaque bipedal locomotion.

Correlation coefficients and phase shifts between pairs of elevation angles are presented in Table 3. The correlation between foot and shank elevation angles was significantly smaller in quail bipedal locomotion (0.76–0.83) than in both macaque (0.88–0.91) and human (0.94–0.97) bipedal locomotion (P<0.001 for all combinations), indicating that the strong correlation between foot and shank elevation angles observed in humans (Hicheur et al., 2006) was not observed in quails. However, the correlation between thigh and foot elevation angles was significantly larger in quail (0.85–0.95) and macaque (0.76–0.92) bipedal locomotion than in human bipedal locomotion (0.24–0.58; P<0.001 for all combinations), and the correlation between shank and thigh elevation angles was significantly larger in quail (0.61–0.87) and macaque (0.77–0.82) bipedal locomotion than in human bipedal locomotion (0.49–0.69; P<0.001 for all combinations).

The phase shift in elevation angle between the foot and the shank ($\Delta\varphi_{FS}$) and between the shank and the thigh ($\Delta\varphi_{ST}$) are both positive in human and macaque bipedal locomotion (Ogihara et al., 2012), indicating that the phase of the shank and the phase of the thigh always precede those of the foot and shank, respectively. However, in quail bipedal locomotion, $\Delta\varphi_{FS}$ was negative, indicating that the phase of the foot preceded that of the shank. However, the magnitude of the phase shift between the foot and the shank in quail bipedal locomotion (13–27 deg) was similar to that of macaque and human bipedal locomotion (6–20 deg), indicating that the phase difference between the foot and shank elevation angles was fairly similar across the three species. By contrast, $\Delta\varphi_{ST}$ in quail bipedal locomotion (3–27 deg) was similar to that in macaque bipedal locomotion (7–18 deg) but significantly smaller than that in human bipedal locomotion (35–50 deg; P<0.001 for all combinations). Therefore, fluctuations in the elevation angles of the three segments differed to a lesser extent in quail locomotion than in human walking.

DISCUSSION

This study demonstrates that a strong planar constraint of inter-segmental coordination is present during bipedal locomotion in quails. Moreover, the degree of planarity of the three-dimensional

Table 1. Cycle duration, duty ratio and Froude number (Fr) of bipedal locomotion in quails

Quail ID	Mass (g)	Sex	Belt speed (m s⁻¹)	N	Cycle duration (s)	Stance duration (s)	Duty ratio	Effective leg length (m)	Fr
1	220	F	0.40	10	0.37±0.020	0.26±0.016	0.71±0.029	0.096	0.17
			0.60	10	0.31±0.010	0.21±0.017	0.69±0.040	0.097	0.38
			0.75	10	0.28±0.004	0.17±0.007	0.60±0.024	0.090	0.64
2	202	F	0.40	10	0.36±0.014	0.24±0.018	0.67±0.031	0.092	0.18
			0.60	10	0.30±0.027	0.19±0.020	0.63±0.028	0.088	0.42
			0.75	10	0.26±0.015	0.16±0.016	0.61±0.032	0.088	0.65
5	204	M	0.40	10	0.39±0.013	0.25±0.013	0.63±0.023	0.085	0.19
			0.60	9	0.33±0.017	0.18±0.023	0.55±0.046	0.087	0.42
8	202	M	0.60	10	0.31±0.006	0.20±0.009	0.66±0.022	0.088	0.44
9	225	M	0.40	8	0.42±0.027	0.30±0.023	0.71±0.012	0.085	0.19

Cycle duration, stance duration and duty ratio are all means ± s.d. N, number of gait cycles.
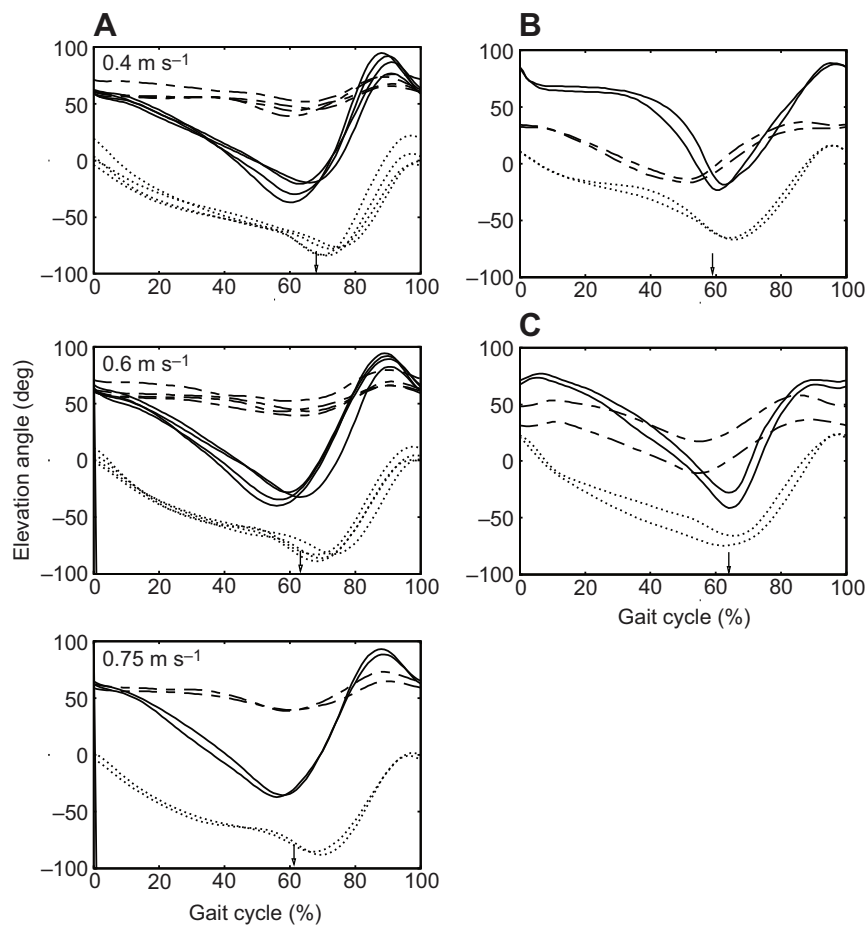
Fig. 1. Elevation angle profiles during bipedal locomotion in quails, humans and macaques.
(A) Mean elevation angle profiles during bipedal locomotion in quails. Curves were averaged across all cycles for each subject and each speed (N=4 subjects for 0.4 m s^{-1}, Fr=0.2; N=4 subjects for 0.6 m s^{-1}, Fr=0.4; and N=2 subjects for 0.75 m s^{-1}, Fr=0.6). 0%, right foot contact; 100%, next foot contact of the same limb. Solid lines, foot; dotted lines, shank; dashed lines, thigh. (B,C) Mean elevation angle profiles during human bipedal locomotion at 6 km h^{-1} (1.7 m s^{-1}, Fr=0.33; B) and Japanese macaque bipedal locomotion at 4 km h^{-1} (1.1 m s^{-1}, Fr=0.4; C) are presented for comparison [data obtained from Ogihara et al. (Ogihara et al., 2012)]. The change in elevation angle with speed is much smaller than inter-species differences (Ogihara et al., 2012). Arrows indicate time of foot off.

trajectory of the elevation angles accounted for >99.5% of the total variance in quail bipedal locomotion, which is significantly higher than that in human locomotion. In humans, the planar covariation of inter-segmental coordination is thought to be a consequence of the central nervous system controlling the kinematics of the limb end point using two global variables (orientation and length of the main axis of the limb), thus reducing the number of effective degrees of freedom that require control from three to two (Ivanenko et al., 2007; Ivanenko et al., 2008). Our results suggest that quail bipedal locomotion is controlled in a similar manner.

However, the way quails achieve this planarity appears to be completely different from the approach in humans. In human locomotion, the foot elevation angle is fairly constant during the mid-stance phase because the foot remains in contact with the ground. This characteristic foot elevation angle profile is strongly correlated with the shank elevation angle profile (r=0.94–0.97) (Ogihara et al., 2012), resulting in planar constraint of the inter-segmental coordination (Hicheur et al., 2006). By contrast, the foot elevation angle in quail bipedal locomotion was similar to that in macaque bipedal and quadrupedal (Courtine et al., 2005) locomotion, and started to decrease soon after foot–ground contact. The correlation between the foot and shank elevation angles was much lower than that in humans. The strong planar constraint of the inter-segmental coordination in quail bipedal locomotion emerged mainly because of the small range of the thigh elevation angle. Hence, the direct cosine of the third eigenvector (u_{3t}) was nearly equal to −1. The quails therefore achieved a high planarity of inter-segmental coordination mainly by restraining the thigh movement with respect to the gravity axis. Furthermore, in quail locomotion,

the foot and thigh elevation angles are more strongly correlated (0.85–0.95). This may suggest that the shank segment, but not the thigh segment (Hicheur et al., 2006), is more independently controlled in quail locomotion.

The spatial orientation of the covariation plane also differed between quails and humans, reflecting the difference in the strategy used to achieve high planarity. In both quails and humans (and also in macaques), the signs of the direct cosines of the first eigenvector, u_{1t}, u_{1s} and u_{1f} (where subscripts t, s and f represent thigh, shank and foot, respectively), were all positive and the first eigenvector was directed in nearly the same direction in all three species. The eigenvector represents the mode shape of oscillation of the three elevation angles. Therefore, the first eigenvector represents the basic back-and-forth movement of the entire limb during bipedal locomotion, and this is common for all three species. However, the direction of the second eigenvector was different in quails and humans, resulting in different planar orientation. In humans, the main oscillation mode represented by the second eigenvector was an out-of-phase oscillation of the thigh and foot elevation angle, but in quails and macaques it was an out-of-phase oscillation of the shank and foot elevation angle (Table 2) (Ogihara et al., 2012). This resulted in different planar orientation between quails and humans. The elevation angle profiles in the swing phase (the final 40% of the gait cycle) represent similar in-phase movement of the three segments for all three species. Therefore, the difference in the oscillation pattern of the elevation angles represented by the second eigenvector is probably more related to a difference in the limb kinematics in the stance phase than to any differences in the swing phase.
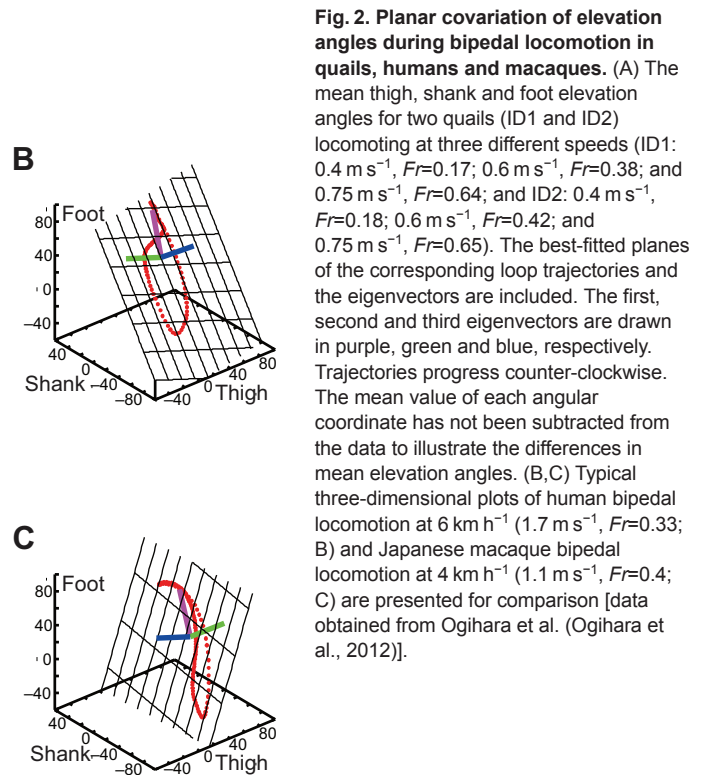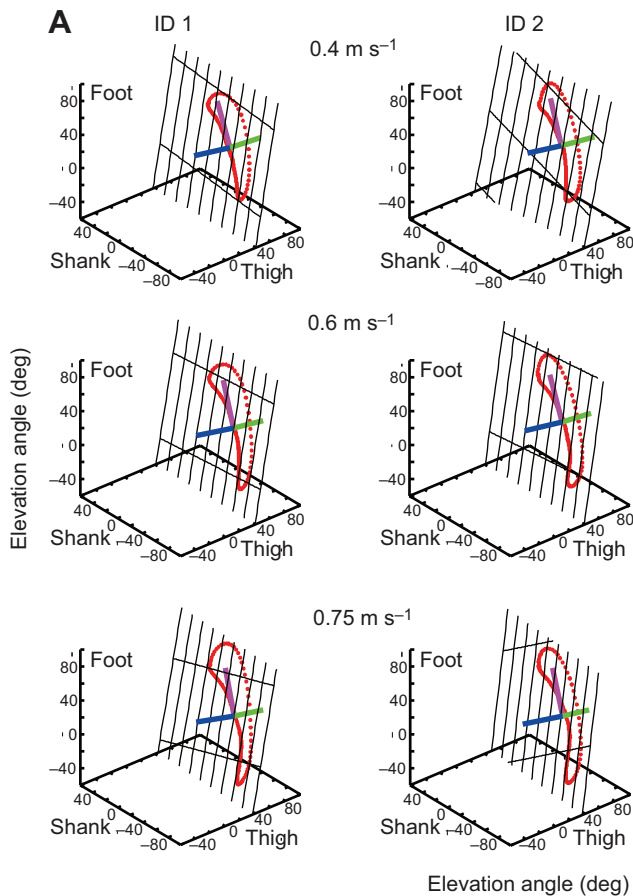
Fig. 2. Planar covariation of elevation angles during bipedal locomotion in quails, humans and macaques. (A) The mean thigh, shank and foot elevation angles for two quails (ID1 and ID2) locomoting at three different speeds (ID1: 0.4 m s^{-1}, Fr=0.17; 0.6 m s^{-1}, Fr=0.38; and 0.75 m s^{-1}, Fr=0.64; and ID2: 0.4 m s^{-1}, Fr=0.18; 0.6 m s^{-1}, Fr=0.42; and 0.75 m s^{-1}, Fr=0.65). The best-fitted planes of the corresponding loop trajectories and the eigenvectors are included. The first, second and third eigenvectors are drawn in purple, green and blue, respectively. Trajectories progress counter-clockwise. The mean value of each angular coordinate has not been subtracted from the data to illustrate the differences in mean elevation angles. (B,C) Typical three-dimensional plots of human bipedal locomotion at 6 km h^{-1} (1.7 m s^{-1}, Fr=0.33; B) and Japanese macaque bipedal locomotion at 4 km h^{-1} (1.1 m s^{-1}, Fr=0.4; C) are presented for comparison [data obtained from Ogihara et al. (Ogihara et al., 2012)].

In human locomotion, the body center of mass (CoM) vaults over the relatively stiff supporting leg, being elevated at the mid-stance phase and lowered in the double-support phase. Horizontal velocity reaches minimum at the mid-stance phase and is maximum in the double-support phase, and potential and kinetic energy therefore fluctuate out of phase, resulting in high walking efficiency. This mutual exchange of two types of mechanical energy is called the inverted-pendulum mechanism and is considered the fundamental mechanism of energy conservation in human bipedal locomotion (Cavagna et al., 1977; Ortega and Farley, 2005; Massaad et al., 2007). The characteristic two-peaked profile of the vertical ground reaction force in human locomotion is linked to the vertical oscillation of the CoM and hence to the efficient utilization of pendular mechanics (Cavagna et al., 1977). It has been suggested

that the quail adopts grounded running, i.e. bipedal gait, utilizing spring-like running mechanics, even though the duty factor is >0.5 (Reilly, 2000). Andrada et al. (Andrada et al., 2013) found that the percentage congruity (Ahn et al., 2004) between the potential and kinetic energy in quail bipedal locomotion was >50% if velocity was >0.5 m s^{-1}, indicating that quails utilized spring-like running mechanics rather than pendular mechanics even at relatively low speeds because their legs are relatively more compliant than human legs (Andrada et al., 2013). It has recently been suggested that macaques also utilize running mechanics in bipedal gait because of their compliant limb morphology (Ogihara et al., 2010). The vertical ground reaction force profile of macaque bipedal locomotion has a single peak, with the peak appearing relatively early in the stance phase (Ogihara et al., 2007; Ogihara et al., 2010). This force profile

Table 2. Eigenvectors of the covariance matrix of elevation angles and corresponding percentage variance

Quail ID	Belt speed (m s^{-1})	1st eigenvector			2nd eigenvector			3rd eigenvector			% Variance		
		u_t	u_s	u_f	u_t	u_s	u_f	u_t	u_s	u_f	i=1	i=2	i=3
1	0.4	0.137	0.580	0.801	0.116	−0.813	0.568	−0.982	−0.014	0.180	88.9±3.8	10.8±3.8	0.3±0.1
2		0.148	0.526	0.836	0.168	−0.845	0.501	−0.970	−0.067	0.213	90.6±0.7	8.8±0.4	0.6±0.3
5		0.164	0.549	0.819	0.008	−0.831	0.555	−0.986	0.084	0.140	91.6±0.8	8.2±0.8	0.1±0.1
9		0.172	0.592	0.787	0.169	−0.805	0.568	−0.970	−0.035	0.238	91.7±0.6	8.0±0.7	0.3±0.1
1	0.6	0.164	0.526	0.834	0.083	−0.849	0.518	−0.981	0.016	0.183	90.5±1.6	9.2±1.6	0.2±0.1
2		0.137	0.547	0.824	0.066	−0.833	0.539	−0.982	0.021	0.151	90.8±2.4	8.9±2.3	0.3±0.2
5		0.164	0.530	0.831	0.028	−0.844	0.533	−0.985	0.064	0.154	90.8±1.0	9.0±1.0	0.2±0.2
8		0.173	0.552	0.815	0.001	−0.827	0.561	−0.984	0.096	0.144	89.6±1.2	10.3±1.1	0.1±0.1
1	0.75	0.191	0.501	0.844	0.056	−0.863	0.499	−0.978	0.048	0.193	90.5±1.0	9.1±0.9	0.4±0.1
2		0.155	0.514	0.843	−0.011	−0.850	0.521	−0.985	0.092	0.127	89.9±1.3	9.8±1.3	0.3±0.3

See Table 2 in Ogihara et al. (Ogihara et al., 2012) for comparisons with human and macaque data. For eigenvectors u_t, u_s and u_f, subscripts t, s and f represent thigh, shank and foot, respectively.

Table 3. Correlation coefficients (*r*) and phase shifts (Δφ) between pairs of elevation angles

Quail ID	Belt speed (m s^{-1})	r_{FS}	r_{ST}	r_{FT}	$\Delta\varphi_{FS}$	$\Delta\varphi_{ST}$
1	0.4	0.767±0.068	0.673±0.132	0.905±0.047	−25.1±6.6	20.8±17.3
2		0.796±0.014	0.613±0.150	0.852±0.116	−18.6±4.0	26.6±25.4
5		0.808±0.021	0.868±0.044	0.951±0.020	−18.1±6.4	9.2±10.1
9		0.830±0.014	0.752±0.039	0.947±0.018	−13.1±3.6	19.6±8.8
1	0.6	0.783±0.034	0.766±0.079	0.944±0.023	−19.2±4.4	12.0±6.4
2		0.798±0.047	0.731±0.121	0.864±0.138	−19.2±6.8	8.6±21.2
5		0.788±0.022	0.826±0.050	0.942±0.042	−18.3±4.9	13.6±10.1
8		0.766±0.022	0.867±0.033	0.947±0.018	−27.0±4.1	14.7±3.8
1	0.75	0.775±0.019	0.777±0.065	0.930±0.020	−24.2±3.7	12.4±5.7
2		0.764±0.028	0.822±0.034	0.904±0.064	−18.5±3.8	3.0±12.4

Subscripts FS, ST and FT denote elevation angles between foot and shank, shank and thigh, and foot and thigh, respectively. *r* and φ data are means ± s.d. See Table 3 in Ogihara et al. (Ogihara et al., 2012) for comparisons with human and macaque data.

is very similar to that of quail ground running (Andrada et al., 2013), suggesting that macaques and quails both utilize spring-like running mechanics rather than pendular mechanics during bipedal gait. The difference in the orientation of the covariance plane could thus be attributable to a difference in the stiffness of the stance leg, and hence to the biomechanical principles utilized during bipedal locomotion (Cappellini et al., 2010). Furthermore, in humans the trunk orientation is almost vertical (orthograde) and the CoM is positioned above the hip joint. In contrast, in quails the trunk orientation is almost horizontal (pronograde) and the CoM is located anterior to the hip joint. This difference in the mechanical characteristics between humans and quails could also account for the difference in the limb kinematics and hence the orientation of the covariance plane.

It is not clear whether the planar covariation of inter-segmental coordination reflects mainly biomechanical factors or the underlying neural control strategy (Hicheur et al., 2006; Ivanenko et al., 2008; Barliya et al., 2009; Ogihara et al., 2012). The results of the present study suggest that, in quail bipedal locomotion, the planar covariance of segment elevation angles was realized by restraining the movement of the thigh segment. It is currently unclear whether the restrained movement of the thigh segment occurs as a result of neuronal control or biomechanical constraint. However, even if the kinematic constraint may have originated from biomechanical factors, such coordinated kinematic synergies could certainly be exploited by the nervous system for control of locomotion. It is of high interest that two extant habitual bipedal species both exhibited strong planar constraint of the inter-segmental coordination during bipedal locomotion, even though they substantially differ in evolutionary history and musculoskeletal anatomy. The convergent evolution of human and avian bipedalism strongly supports the functional significance of the planar kinematic synergies for control of locomotion, regardless of whether it reflects simplified neuronal control or biomechanical constraint.

MATERIALS AND METHODS

Five adult common quails (*C. coturnix*) locomoted on a treadmill at 0.4, 0.6 and 0.75 m s^{-1} and were recorded using X-ray cineradiography (Neurostar, Siemens, Erlangen, Germany) at the Institut für Spezielle Zoologie und Evolutionsbiologie mit Phyletischem Museum, Germany. X-ray recordings were taken from the lateral projection. The tube voltage, current and sampling frequency were 40 kV, 53 mA and 500 Hz, respectively. From the motion images, well-recorded bipedal sequences were extracted and corrected for distortion prior to analysis. Five landmarks (hip joint, knee joint, intertarsal joint, tarsometatarso-phalangeal joint and tip of middle toe; Fig. 3) on the right-hand side of the body were manually digitized on at least every tenth frame using SimiMotion software (Simi Reality Systems, Unterschleißheim,

Germany). More frames were digitized around the time of touch-down and lift-off to ensure that the kinematics were precisely captured. Kinematic analysis based on the X-ray fluoroscopic system is confirmed to be more accurate than the conventional external marker-based approach as the X-ray fluoroscopy allows direct identification of the joint positions and avoids errors introduced by skin movement (Bauman and Chang, 2010). The change in position of each coordinate over time was low-pass filtered at 21 Hz using a zero-phase shift digital low-pass filter. Cycle duration, stance phase duration (foot contact time) and duty factor (stance phase duration/cycle duration) of each digitized cycle were calculated from the recorded data. Gait cycles in which the birds moved too slow or too fast relative to the belt speed were excluded from the analyses. Two subjects (1 and 2) locomoted on the treadmill at all three speeds and the other three subjects locomoted at one or two of the three speeds: subject 5 locomoted at 0.4 and 0.6 m s^{-1}, subject 8 locomoted only at 0.6 m s^{-1} and subject 9 locomoted only at 0.4 m s^{-1} (Table 1).

Elevation angles of the thigh (femur), shank (tibiotarsus) and foot (tarsometatarsus) segments were calculated as the angles of the corresponding limbs with respect to the vertical axis (Fig. 3). Calculated angle profiles were interpolated over the cycle duration to fit a 100-point time base for normalization of the time. Time courses of the elevation angles were then plotted in a three-dimensional space and trajectories were fitted by a plane using a least-squares method (Borghese et al., 1996). For this purpose, principal component analysis of the covariance matrix of the elevation angles was performed using MATLAB (The MathWorks, Natick, MA, USA). As reported in prior studies, the covariance matrix based on non-normalized angles was used in the principal component analysis. The first two eigenvectors describe the best-fitting plane and the third vector represents the orientation of the plane. The direction cosines of the *i*th eigenvector with the positive axis of the thigh, shank and foot elevation angles are denoted as u_{it}, u_{is} and u_{if}, respectively. These values were used to quantify the differences in directions of the eigenvectors. The variance accounted for by the *i*th eigenvector is expressed by its percentage variance;
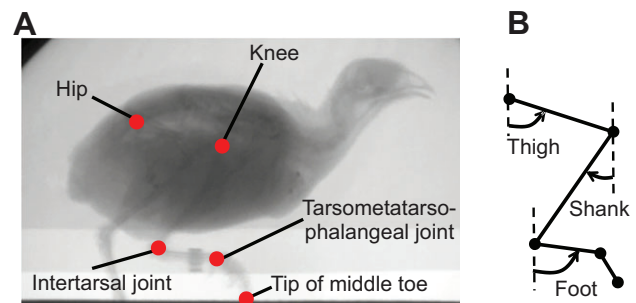

Fig. 3. Measurement of bipedal locomotion in quails. (A) Two-dimensional coordinates of five landmarks on the right leg were monitored using the X-ray fluoroscopic system. (B) Definition of elevation angles. Elevation angles increased during counter-clockwise rotation of the segment with respect to the vertical axis.

that is, the proportion of the ith eigenvalue compared with the sum of the three eigenvalues. The planarity of the trajectories was quantified by the sum of the percentage variances of the first and second eigenvectors. A third eigenvalue of zero was equivalent to 100% planarity. For further details of the calculation method, see previous publications (Borghese et al., 1996; Grasso et al., 2000; Ivanenko et al., 2008).

To evaluate similarities between pairs of elevation angles, correlation coefficients were calculated as described elsewhere (Hicheur et al., 2006). Elevation angle profiles were approximated using the first Fourier decomposition harmonics to quantify phase shifts between pairs of elevation angles (Bianchi et al., 1998; Barliya et al., 2009).

Temporal changes in segment elevation angles during human and macaque bipedal locomotion were taken from previously published data for comparison (Ogihara et al., 2012). Briefly, adult humans and macaques locomoting on a treadmill were recorded at 100 Hz using a motion capture system and at 125 Hz using high speed cameras, respectively, to calculate elevation angles.

For appropriate comparisons of bipedal locomotion among the three species, we calculated the Froude number, defined as $Fr=v^2/gL$, where v is the velocity, g is the gravitational acceleration and L is the effective leg length defined as the mean distance between the hip and the tarsometatarso-phalangeal joint during the stance phase (Ogihara et al., 2010). Analysis of variance and *post hoc* Tukey's honestly significant difference multiple comparisons tests were performed using Statistica 10 software (StatSoft, Tulsa, OK, USA) to test for significant differences in the percentage variances, directions of the eigenvectors, correlation coefficients and phase shifts.

Author contributions
N.O., E.A. and J.A.N. conceived and designed the study, T.O., E.A. and J.A.N. performed the experiments, N.O. and T.O. performed data analysis, N.O. drafted the manuscript, and all authors edited and approved the manuscript prior to submission.

References

Abourachid, A. and Renous, S. (2000). Bipedal locomotion in ratites (Paleognatiform): examples of cursorial birds. *Ibis* **142**, 538-549.

Abourachid, A., Hackert, R., Herbin, M., Libourel, P. A., Lambert, F., Gioanni, H., Provini, P., Blazevic, P. and Hugel, V. (2011). Bird terrestrial locomotion as revealed by 3D kinematics. *Zoology* **114**, 360-368.

Ahn, A. N., Furrow, E. and Biewener, A. A. (2004). Walking and running in the red-legged running frog, *Kassina maculata*. *J. Exp. Biol.* **207**, 399-410.

Andrada, E., Nyakatura, J. A., Bergmann, F. and Blickhan, R. (2013). Adjustments of global and local hindlimb properties during terrestrial locomotion of the common quail (*Coturnix coturnix*). *J. Exp. Biol.* **216**, 3906-3916.

Barliya, A., Omlor, L., Giese, M. A. and Flash, T. (2009). An analytical formulation of the law of intersegmental coordination during human locomotion. *Exp. Brain Res.* **193**, 371-385.

Bauman, J. M. and Chang, Y. H. (2010). High-speed X-ray video demonstrates significant skin movement errors with standard optical kinematics during rat locomotion. *J. Neurosci. Methods* **186**, 18-24.

Bianchi, L., Angelini, D., Orani, G. P. and Lacquaniti, F. (1998). Kinematic coordination in human gait: relation to mechanical energy cost. *J. Neurophysiol.* **79**, 2155-2170.

Borghese, N. A., Bianchi, L. and Lacquaniti, F. (1996). Kinematic determinants of human locomotion. *J. Physiol.* **494**, 863-879.

Cappellini, G., Ivanenko, Y. P., Dominici, N., Poppele, R. E. and Lacquaniti, F. (2010). Migration of motor pool activity in the spinal cord reflects body mechanics in human locomotion. *J. Neurophysiol.* **104**, 3064-3073.

Cavagna, G. A., Heglund, N. C. and Taylor, C. R. (1977). Mechanical work in terrestrial locomotion: two basic mechanisms for minimizing energy expenditure. *Am. J. Phys. Physiol.* **233**, R243-R261.

Courtine, G., Roy, R. R., Hodgson, J., McKay, H., Raven, J., Zhong, H., Yang, H., Tuszynski, M. H. and Edgerton, V. R. (2005). Kinematic and EMG determinants in quadrupedal locomotion of a non-human primate (Rhesus). *J. Neurophysiol.* **93**, 3127-3145.

Dominici, N., Ivanenko, Y. P., Cappellini, G., Zampagni, M. L. and Lacquaniti, F. (2010). Kinematic strategies in newly walking toddlers stepping over different support surfaces. *J. Neurophysiol.* **103**, 1673-1684.

Fujita, M. (2004). Kinematic parameters of the walking of herons, ground-feeders, and waterfowl. *Comp. Biochem. Physiol.* **139A**, 117-124.

Gatesy, S. M. (1999). Guineafowl hind limb function. I: Cineradiographic analysis and seed effects. *J. Morphol.* **240**, 115-125.

Gatesy, S. M. and Biewener, A. A. (1991). Bipedal locomotion: effect of speed, size and limb posture in birds and humans. *J. Zool. (Lond.)* **224**, 127-147.

Grasso, R., Bianchi, L. and Lacquaniti, F. (1998). Motor patterns for human gait: backward versus forward locomotion. *J. Neurophysiol.* **80**, 1868-1885.

Grasso, R., Zago, M. and Lacquaniti, F. (2000). Interactions between posture and locomotion: motor patterns in humans walking with bent posture versus erect posture. *J. Neurophysiol.* **83**, 288-300.

Hancock, J. A., Stevens, N. J. and Biknevicius, A. R. (2007). Whole-body mechanics and kinematics of terrestrial locomotion in the elegant-crested tinamou *Eudromia elegans. Ibis* **149**, 605-614.

Hicheur, H., Terekhov, A. V. and Berthoz, A. (2006). Intersegmental coordination during human locomotion: does planar covariation of elevation angles reflect central constraints? *J. Neurophysiol.* **96**, 1406-1419.

Hutchinson, J. R. and Gatesy, S. M. (2001). Bipedalism. In *Encyclopedia of Life Sciences.* London: Nature Publishing Group.

Ivanenko, Y. P., Grasso, R., Macellari, V. and Lacquaniti, F. (2002). Control of foot trajectory in human locomotion: role of ground contact forces in simulated reduced gravity. *J. Neurophysiol.* **87**, 3070-3089.

Ivanenko, Y. P., Dominici, N., Cappellini, G. and Lacquaniti, F. (2005). Kinematics in newly walking toddlers does not depend upon postural stability. *J. Neurophysiol.* **94**, 754-763.

Ivanenko, Y. P., Cappellini, G., Dominici, N., Poppele, R. E. and Lacquaniti, F. (2007). Modular control of limb movements during human locomotion. *J. Neurosci.* **27**, 11149-11161.

Ivanenko, Y. P., d'Avella, A., Poppele, R. E. and Lacquaniti, F. (2008). On the origin of planar covariation of elevation angles during human locomotion. *J. Neurophysiol.* **99**, 1890-1898.

Leurs, F., Bengoetxea, A., Cebolla, A. M., De Saedeleer, C., Dan, B. and Cheron, G. (2012). Planar covariation of elevation angles in prosthetic gait. *Gait Posture* **35**, 647-652.

Massaad, F., Lejeune, T. M. and Detrembleur, C. (2007). The up and down bobbing of human walking: a compromise between muscle work and efficiency. *J. Physiol.* **582**, 789-799.

Muir, G. D., Gosline, J. M. and Steeves, J. D. (1996). Ontogeny of bipedal locomotion: walking and running in the chick. *J. Physiol.* **493**, 589-601.

Noble, J. W. and Prentice, S. D. (2008). Intersegmental coordination while walking up inclined surfaces: age and ramp angle effects. *Exp. Brain Res.* **189**, 249-255.

Nyakatura, J. A., Andrada, E., Grimm, N., Weise, H. and Fischer, M. S. (2012). Kinematics and center of mass mechanics during terrestrial locomotion in northern lapwings (*Vanellus vanellus*, Charadriiformes). *J. Exp. Zool. A* **317**, 580-594.

Ogihara, N., Hirasaki, E., Kumakura, H. and Nakatsukasa, M. (2007). Ground-reaction-force profiles of bipedal walking in bipedally trained Japanese monkeys. *J. Hum. Evol.* **53**, 302-308.

Ogihara, N., Makishima, H. and Nakatsukasa, M. (2010). Three-dimensional musculoskeletal kinematics during bipedal locomotion in the Japanese macaque, reconstructed based on an anatomical model-matching method. *J. Hum. Evol.* **58**, 252-261.

Ogihara, N., Kikuchi, T., Ishiguro, Y., Makishima, H. and Nakatsukasa, M. (2012). Planar covariation of limb elevation angles during bipedal walking in the Japanese macaque. *J. R. Soc. Interface* **9**, 2181-2190.

Ortega, J. D. and Farley, C. T. (2005). Minimizing center of mass vertical movement increases metabolic cost in walking. *J. Appl. Physiol.* **99**, 2099-2107.

Reilly, S. M. (2000). Locomotion in the quail (*Coturnix japonica*): the kinematics of walking and increasing speed. *J. Morphol.* **243**, 173-185.

Rubenson, J., Lloyd, D. G., Besier, T. F., Heliams, D. B. and Fournier, P. A. (2007). Running in ostriches (*Struthio camelus*): three-dimensional joint axes alignment and joint kinematics. *J. Exp. Biol.* **210**, 2548-2562.

Stoessel, A. and Fischer, M. S. (2012). Comparative intralimb coordination in avian bipedal locomotion. *J. Exp. Biol.* **215**, 4055-4069.

Sylos-Labini, F., Ivanenko, Y. P., Cappellini, G., Portone, A., MacLellan, M. J. and Lacquaniti, F. (2013). Changes of gait kinematics in different simulators of reduced gravity. *J. Mot. Behav.* **45**, 495-505.